Injection-locked fiber laser for tunable millimeter-wave generation

Shilong Pan,[1,*] Zhenzhou Tang,[1] Dan Zhu,[1] De Ben,[1] and Jianping Yao[1,2]

[1]*College of Electronic and Information Engineering, Nanjing University of Aeronautics and Astronautics, Nanjing, 210016, China*

[2]*Microwave Photonics Research Laboratory, School of Information Technology and Engineering, University of Ottawa, Ottawa, ON K1N 6N5, China*

**Corresponding author: pans@nuaa.edu.cn*

Received August 23, 2011; revised October 5, 2011; accepted October 31, 2011; posted November 3, 2011 (Doc. ID 153273); published December 9, 2011

A dual-ring injection-locked fiber laser consisting of a ring of optoelectronic oscillator (OEO) and a ring of fiber laser is proposed and demonstrated for tunable millimeter-wave (mm-wave) generation. The approach combines the advantages of mm-wave generation based on OEOs and fiber lasers, which can generate a high-frequency, low-phase-noise, and a mode-hopping-free mm-wave signal with a large tuning range. A low-phase-noise mm-wave signal with a tunable frequency of 30–50 GHz and a tuning step of 10 GHz is obtained in a proof-of-concept experiment. The tuning range can be as large as 140 GHz if a high bandwidth photodetector is applied.

OCIS codes: 350.4010, 140.3510, 140.3520.

Photonic generation of frequency-tunable millimeter-wave (mm-wave) signals is of great interest for numerous applications, such as radio over fiber system, antenna remoting, radar, software defined radio, and modern instrumentation [1]. The basic idea of the photonic approaches to generate the high-quality mm-wave signal is to heterodyne two optical waves at a photomixer or photodetector (PD) with a wavelength difference that falls in the mm-wave range [2]. To reduce the phase noise of the generated mm-wave signal, it is essential that the two optical waves applied to the photomixer or PD for heterodyne are phase correlated. Numerous techniques have been proposed in the last few decades to lock the two optical waves in phase. These techniques can be classified into five categories: (1) dual-wavelength laser source [3–5], (2) optical phase-locked loop [6,7], (3) optical injection locking [7,8], (4) external modulation [9,10] and (5) optoelectronic oscillator (OEO) [11,12]. Photonic mm-wave generation based on a dual-wavelength laser can achieve a large tuning range, but complicated schemes are needed to suppress the multimode oscillation and mode hopping. On the other hand, OEOs can be used as a high-quality mm-wave source, but the tuning range is limited in principle by the high-Q bandpass filter in the cavity. In addition, the maximum operational frequency of an OEO is restricted by the bandwidth of the electronic components and the electro-optic modulator. Other methods, such as optical phase-locked loop, optical injection locking, and external modulation, can also generate a high-frequency mm-wave, but they require a high-quality microwave or mm-wave reference, which is complicated and costly.

In this Letter, we propose and demonstrate a novel approach to generate a frequency-tunable mm-wave signal based on a dual-ring architecture, which consists of a polarization-modulator-(PolM)-based OEO and a fiber laser that is injection locked by one sideband of the optical output of the OEO. The proposed scheme combines the advantages of both OEO and fiber laser, which can generate a high-quality mm-wave with a large tuning range. An experiment is performed. A high-quality mm-wave signal with a tunable frequency of 30–50 GHz and a tuning step of 10 GHz, restricted only by the bandwidth of the PD used in the experiment, is generated. The scheme is potentially operated to generate a 140 GHz signal if a PD with a high bandwidth is applied.

Figure 1 shows the schematic diagram of the proposed dual-ring injection-locked fiber laser, which is composed of a PolM-based OEO and a fiber laser. The OEO is constructed from a tunable laser source (TLS), a PolM, two polarization controllers (PC1 and PC2), a polarizer, a PD, an electrical amplifier (EA), and an electrical bandpass filter (EBPF). The PolM is a special phase modulator that can support both TE and TM modes with opposite phase modulation indices. The PolM in conjunction with PC2 and the polarizer is equivalent to an intensity modulator (IM) [12], which is biased at the quadrature transmission point by properly setting PC1 and PC2. In the fiber laser, an erbium-doped fiber amplifer (EDFA) is used to provide the optical gain. A circulator connected to a fiber Bragg grating (FBG) is incorporated for wavelength

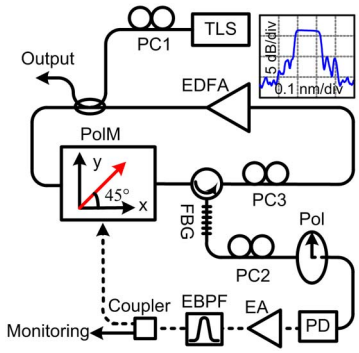

Fig. 1. (Color online) Schematic diagram of the dual-ring injection-locked fiber laser for mm-wave generation. TLS: tunable laser source; PolM: polarization modulator; PC: polarization controller; FBG: fiber Bragg grating; EDFA: erbium-doped fiber amplifer; Pol: polarizer; PD: photodetector; EA: electrical amplifier; EBPF: electrical bandpass filter. Inset: the transmission response of the FBG.

selection. The 3 dB bandwidth of the reflection response of the FBG is chosen to be very narrow (~0.14 nm), and the central wavelength is selected to be far (>0.24 nm) away from the wavelength of the TLS. Therefore, the optical carrier from the TLS is suppressed by the reflection response of the FBG, so it will not significantly affect the fiber laser. On the other hand, the lightwave from the fiber laser is greatly attenuated by the transmission response of the FBG, so it will not affect the oscillation of the OEO either. A 2×2 optical coupler is used for laser output, which is also used to combine the lightwaves from the TLS and from the fiber laser. A third PC (PC3) is inserted in the fiber ring for performance optimization.

The pump current of the EDFA is controlled to let the net gain of the fiber laser be a little smaller than unity. When the TLS is shut down, both the OEO and the fiber laser cannot oscillate, because the net gains of both rings are smaller than unity. When the TLS is switched on, the OEO starts to oscillate at one of its eigenmodes, which is determined by the central frequency of the EBPF. The oscillation signal in the OEO is then fed back to the RF port of the PolM, generating a lot of sidebands around the optical carrier. The wavelength of the TLS is adjusted to ensure that one sideband drops in the pass band of the reflection response of the FBG, making the net gain of a longitudinal mode in the fiber laser larger than unity. Thus, the fiber laser is injection locked, which suppresses effectively the multimode oscillation and mode hopping that is common in a conventional free-running fiber laser. In addition, the lasing wavelength of the fiber laser and the optical carrier from the TLS are phase correlated, which can be used to generate a high-quality mm-wave at a PD. The frequency tuning can be realized by adjusting the wavelength of the TLS with a tuning step that is determined by the oscillation frequency of the OEO. The tuning range is related to the saturation output power of the EA used in the OEO, because a larger electrical power introduced to the PolM would stimulate more and stronger sidebands, and thus support injection locking of the fiber laser with a lasing wavelength that is far from the wavelength of the TLS. It should be noted that the polarization modulation in the PolM would also generate a lot of sidebands around the oscillating wavelength of the fiber laser, but this will not cause an evident problem for the generation of the mm-wave signal because (1) the 3 dB bandwidth of the FBG is narrow enough to suppress most of the sidebands, and (2) the polarization modulation is a kind of phase modulation, so the sidebands would not generate a frequency component when detected at a PD. In addition, mode-locking of the fiber laser at the OEO oscillation frequency is also avoided because of the effective suppression of the sidebands by the FBG.

A proof-of-concept experiment is carried out to verify the proposed approach. The key parameters used in the experiment are as follows: the bandwidth and half-wave voltage of the PolM (Versawave PL-40G-3-1550) is 40 GHz and 3.5 V; the PD in the OEO has a 3 dB bandwidth of 10 GHz and a responsivity of 0.85 A/W; the bandwidth of the EBPF is 10 MHz centered at 10 GHz; the gain of the EA is about 55 dB; the free spectral range (FSR) of the OEO is measured to be 4.02 MHz, corresponding to a cavity length of ~50 m; the central wavelength, the 3 dB bandwidth, and the reflectivity of the FBG are 1548.45 nm, 0.14 nm, and 99.9%, respectively. A second PD with a bandwidth of 40 GHz is inserted at the output of the fiber laser for heterodyning the two phase-correlated optical waves. The cavity length of the fiber laser is about 44.6 m. The optical signal is monitored by an optical spectrum analyzer (Ando AQ 6317B) with a resolution of 0.01 nm, and the generated mm-wave signal is observed by an electrical spectrum analyzer (ESA, Agilent E4448A, 3 Hz–50 GHz).

Figure 2 shows the experimental results when the scheme is configured to generate a 40 GHz mm-wave signal. The wavelength of the optical carrier from the TLS is set at 1548.12 nm. As can be seen from the optical spectrum observed at the output of the scheme (Fig. 2(a)), the oscillation wavelength of the fiber laser is 1548.44 nm, which is injection locked at the fourth sideband of the polarization-modulated optical carrier from the TLS. Because of the polarization modulation in the PolM and the insufficient rejection ratio in the reflection response of the FBG, small sidebands appear around 1548.12 nm and 1548.44 nm. Since 1548.12 nm is farther away from the central wavelength of the FBG, the sidebands around 1548.12 nm are much weaker than those around 1548.44 nm. If an FBG with narrower bandwidth and steeper edge is applied, the power of the undesirable sidebands would be further reduced. Figure 2(b) shows the electrical spectrum of the generated mm-wave signal. A spectral line at 40 GHz is obtained, which is more than

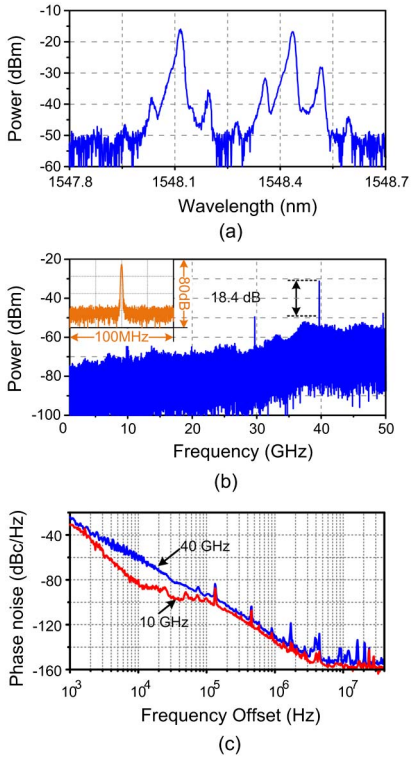

Fig. 2. (Color online) (a) The optical spectrum of the two phase-correlated optical waves. (b) The electrical spectrum of the generated mm-wave signal (inset: enlarged view of the 40 GHz signal at SPAN = 100 MHz and RBW = 910 kHz). (c) The single sideband (SSB) phase noise spectrum when the scheme is configured to generate a 40 GHz mm-wave signal.

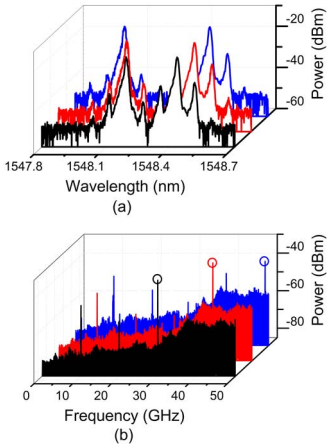

Fig. 3. (Color online) The spectra of (a) the optical signal and (b) the generated electrical signal, tuned from 30 GHz to 50 GHz.

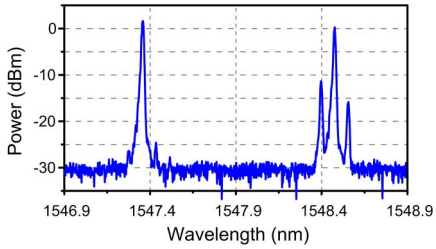

Fig. 4. (Color online) The optical spectrum of the two phase-correlated optical waves with a wavelength difference of 140 GHz.

18 dB higher than the 10- and 30 GHz components. Since the PD has a 3 dB loss at 40 GHz as compared with that at the frequency below 30 GHz, the extinction ratio is actually larger than 20 dB. The enlarged view of the 40 GHz signal is shown in the inset of Fig. 2(b). No multimode oscillation is observed. The phase noise performance of the generated mm-wave signal is studied. As shown in Fig. 2(c), the 40 GHz signal has a phase noise of −130 dBc/Hz at 1 MHz offset frequency, which has a phase noise degradation of ~6 dB as compared with that of the 10 GHz OEO oscillation signal, much less than the ideal phase noise degradation (12 dB) for a frequency-quadrupling signal, showing that the injection locking evidently improves the phase noise performance of the generated signal. The phase noise can be further reduced if a high-performance OEO [13] is applied. The 40 GHz beat note is observed on the ESA under a span of 10 MHz and a resolution bandwidth of 91 kHz for more than 30 minutes; no mode hopping is observed.

The frequency tuning of the proposed mm-wave generation scheme is also investigated, and it is implemented by simply adjusting the wavelength of the TLS. As shown in Fig. 3, when the wavelength of the TLS is switched from 1548.20, to 1548.12, to 1548.04 nm, the mm-wave beat note at 30, 40, and 50 GHz, respectively, is observed on the ESA. Further tuning the wavelength of the TLS, we can obtain two phase-correlated optical waves with a wavelength difference as large as 140 GHz, as shown in Fig. 4. Because of the limited bandwidth of the PD and the ESA, we can not observe the 140 GHz mm-wave signal. So far, a PD based on a unitravelling carrier structure allows an effective detection of two phase-correlated wavelengths with a wavelength spacing as large as 914 GHz [14]. If that PD is applied, the proposed approach should be able to generate a mm-wave in the subterahertz range.

In conclusion, a dual-ring injection-locked fiber laser was proposed and experimentally demonstrated. The results showed that two phase-correlated optical waves with a wavelength difference as large as 140 GHz were obtained. The wavelength spacing could be tuned with a tuning step of 10 GHz. By beating the two optical waves at a PD, a microwave signal with a switchable frequency from 30 to 50 GHz was generated. The phase noise performance of the generated mm-wave was also studied. The proposed method is free from mode hopping and has a large tuning range, which may find applications in a radio over fiber system, software defined radio, and modern instrumentation.

This work was supported in part by the National Natural Science Foundation of China under grant 61107063, the National Basic Research Program of China (973 Program) under grant 2012CB315705, and the Program for New Century Excellent Talents in University (NCET) under grant NCET-10-0072.

References

1. J. P. Yao, J. Lightwave Technol. **27**, 314 (2009).
2. T. Nagatsuma, IEEE Microw. Mag. **10**, 64 (2009).
3. S. L. Pan and J. P. Yao, Opt. Express **17**, 5414 (2009).
4. X. Y. He, D. N. Wang, and C. R. Liao, J. Lightwave Technol. **29**, 842 (2011).
5. B. Lin, M. Jiang, S. C. Tjin, and P. Shum, IEEE Photon. Technol. Lett. **23**, 1292 (2011).
6. R. J. Steed, L. Ponnampalam, M. J. Fice, C. C. Renaud, D. C. Rogers, D. G. Moodie, G. D. Maxwell, I. F. Lealman, M. J. Robertson, L. Pavlovic, L. Naglic, M. Vidmar, and A. J. Seeds, IEEE J. Sel. Top. Quantum Electron. **17**, 210 (2011).
7. A. C. Bordonalli, C. Walton, and A. J. Seeds, J. Lightwave Technol. **17**, 328 (1999).
8. S. C. Chan, IEEE J. Quantum Electron. **46**, 421 (2010).
9. J. J. O'Reilly, P. M. Lane, R. Heidemann, and R. Hofstetter, Electron. Lett. **28**, 2309 (1992).
10. S. L. Pan and J. P. Yao, IEEE Trans. Microw. Theory Tech. **58**, 1967 (2010).
11. X. S. Yao and L. Maleki, IEEE J. Quantum Electron. **32**, 1141 (1996).
12. S. L. Pan and J. P. Yao, J. Lightwave Technol. **27**, 3531 (2009).
13. E. Shumakher and G. Eisenstein, IEEE Photon. Technol. Lett. **20**, 1881 (2008).
14. C. C. Renaud, M. Robertson, D. Rogers, R. Firth, P. J. Cannard, R. Moore, and A. J. Seeds, in *Millimeter-Wave and Terahertz Photonics* (2006), pp. 61940C-8.